A global assessment of the timing of extreme rainfall from TRMM and GPM for improving hydrologic design

A global assessment of the timing of extreme rainfall from TRMM and GPM for improving hydrologic design

2016 Environ. Res. Lett. 11 054003

(http://iopscience.iop.org/1748-9326/11/5/054003)

Environmental Research Letters

LETTER

A global assessment of the timing of extreme rainfall from TRMM and GPM for improving hydrologic design

Andrea Libertino[1,2,4], **Ashish Sharma**[2], **Venkat Lakshmi**[3] **and Pierluigi Claps**[1]

[1] Department of Environment, Land and Infrastructure Engineering, Politecnico di Torino, Torino I-10129, Italy
[2] School of Civil and Environmental Engineering, The University of New South Wales, Sydney, NSW 2052, Australia
[3] Department of Earth and Ocean Sciences, University of South Carolina, Columbia, SC 29208, USA
[4] Author to whom any correspondence should be addressed.

E-mail: andrea.libertino@polito.it

Keywords: TRMM, GPM, extreme rainfall, precipitation, remote sensing

Supplementary material for this article is available online

OPEN ACCESS

RECEIVED
21 November 2015

REVISED
1 April 2016

ACCEPTED FOR PUBLICATION
4 April 2016

PUBLISHED
25 April 2016

Abstract

The tropical rainfall measuring mission (TRMM) has revolutionized the measurement of precipitation worldwide. However, TRMM significantly underestimates rainfall in deep convection systems, being therefore of little help for the analysis of extreme precipitation depths. This work evaluates the ability of both TRMM and the recently launched global precipitation measurement (GPM) mission to help in the identification of the timing of severe rainfall events. We compare the date of occurrence of the most severe daily rainfall recorded each year by a global rain gauge network with the ones estimated by TRMM. The match rate between the two is found to approach 50%, indicating significant consistency between the two data sources. This figure rises to 60% for GPM, indicating the potential for this new mission to improve the accuracy associated with TRMM. Further efforts are needed in improving the GPM conversion algorithms in order to reduce the bias affecting the estimation of intense depths. The results however show that the timing estimated from GPM can provide a solid basis for an extensive characterization of the spatio-temporal distribution of extreme rainfall in poorly gauged regions of the world.

1. Introduction

Slow-moving thunderstorms [1, 2] lead to extreme rainfall which often causes disruptive floods. Due to the small spatial extension, this type of rainfall system is difficult to sample by using ground rain gauge networks. Even in a dense rain gauge network, such as that of the Liguria region in North-Western Italy (figure 1(a)), the uneven spatial distribution of the network and the complex orography reduce the chances of observing extreme rainstorms. This criticality increases at higher elevations, where the gauge density is smaller. The question that arises is whether remotely sensed rainfall products from radars [3] or satellites [4] can help in reconstructing the spatial features of rainfall extremes in areas with a poor density in stations.

The precipitation radar (PR) operating on the tropical rainfall measuring mission (TRMM) satellite has been used to study storms in the tropics and subtropics [5]. A wide range of studies has evaluated TRMM performances on a global scale (e.g., [6–10]). Alongside numerous positive results, some drawbacks can be pointed out. For instance, some authors have identified a poor TRMM quantification of large precipitation amounts in and near tropical mountainous regions and, in general, in regions characterized by intense deep convection over land (e.g., [11–14]). Moreover, Tian *et al* [15] show an increase in TRMM estimation uncertainty in complex terrains, coastlines and inland water-bodies, cold surfaces, high latitudes and light precipitation. Based on TRMM outcomes, NASA and JAXA deployed the GPM core observatory [16].

This work aims at evaluating the usability of TRMM and Global Precipitation Measurement mission (GPM) data in the study of the spatio-temporal characteristics of severe rainfall. Once the significant

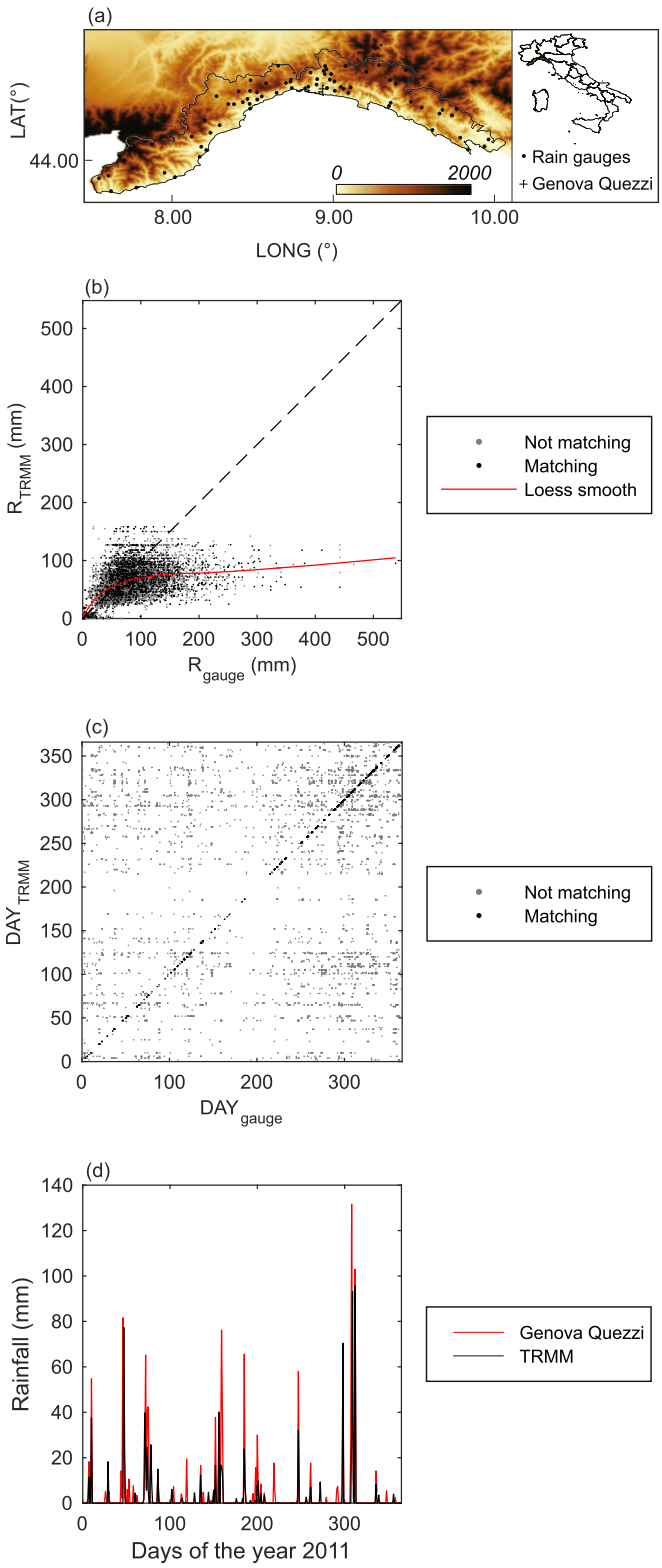

Figure 1. (a) The Liguria region, in North-Western Italy. Orography and localization of the regional rain gauge network. The chromatic scale refers to the altitude in meters above the sea level. (b) Three largest annual daily rainfall recorded at each rain gauge (R_{gauge}) compared with the values of the overlying TRMM cell (R_{TRMM}) in the 1998–2014 period. (c) Temporal distribution along the year of the matching and not-matching three major events. Black dots refer to days ranked likewise in the rain gauge and TRMM series. (d) The 2001 daily rainfall series of the rain gauge 'Genova Quezzi' (44.237° N, 8.9726° E, 200 m a.s.l.) and of the overlying TRMM cell.

bias affecting the magnitude estimation is assessed, we explore the ability to represent the timing of severe storms of satellite products. At first, we test the aforementioned bias considering the three largest daily rainfall depths recorded each year between 1998 and 2014 by the rain gauges of the Liguria regional

network. Results are reported in figure 1(b). An average value of 11% underestimation can be pointed out. Indeed, while a slight overestimation can be recorded for the smaller amounts, the loess curve [17] shows an increasing tendency starting from at-gauge values (R_{gauge}) of around 100 mm. The underestimation reaches values near 100% for the largest rainfall quantities. The average underestimation increases to 16% when only considering gauges above 400 m a.s.l. (the average elevation of the gauge network). More significant differences would be expected if a larger number of gauges were to be available at higher elevations. It is therefore evident that TRMM data are still far from being useful when intense rainfall estimation is the target. They may however provide useful information on the spatio-temporal distribution of extremes.

The timing of the rainfall events considered in the Liguria case study (i.e. the three largest daily rainfall depths recorded each year between 1998 and 2014 by each rain gauge) is shown in panel (c) of figure 1. The timing is uniformly distributed throughout the year, with a low density in the central dry season (i.e. from June to August). In about 25% of the cases, TRMM identifies the correct date of occurrence of each considered event, confirming the findings of other studies (e.g., [18]). If we consider only the rain gauges above 400m a.s.l. there is no significant variation in the match percentage (not shown); this finding possibly denotes a behavior unrelated to elevation. Panel (d) of figure 1 shows the time series of the 'Genova Quezzi' rain gauge during year 2011 along with the signal from the overlying TRMM cell: the satellite correctly identifies the days with intense precipitation, even if underestimating the rainfall amount.

The Liguria region is considered as a challenging introductory case study, as it possesses numerous characteristics that prevent a direct use of TRMM data (e.g., high latitude, complex morphology, etc). However, this work aims at considering the TRMM and GPM performance at the global scale. Therefore, the following questions are investigated: (a) Does the accuracy of the timing of extreme rainfall estimated by satellite vary with latitude? (b) Does this accuracy change with improvement in satellite spatio-temporal resolution and, more specifically, does rainfall data from GPM perform better than data from TRMM? And, (c) how does accuracy vary with GPM spatial resolution?

Positive outcomes of this study are expected to produce added value in stormwater design, even if a statistical characterization of extreme rainfall from satellite data is yet unfeasible. Satellite-derived timing information can help in reconstructing the synoptic influences on the local spatial variability, allowing a systematic analysis of the synoptic configurations concurrent to severe rainfall patterns. This could benefit the estimation of intensity-frequency-duration relationships in ungauged areas and the characterization of extreme rainfall in poorly gauged regions of the world, helping to clarify the connections between large-scale meteorological systems and actual rainfall distribution in space. Furthermore, satellite products can help connecting recorded rainfall with the tracks of severe storms, allowing a high resolution analysis over wide areas, including the seas (e.g., [19]).

Moreover, large scale timing information can be useful in many other fields of the hydrologic sciences which focus on the joint occurrence of severe rainfall and other phenomena (e.g., soil erosion, landslides, etc [20, 21]). In fact, by expanding the analysis at the global scale, satellite data can drastically improve the sample size of these studies with benefits for the robustness of the outcomes.

2. Data and methodology

The assessment of the ability of TRMM and GPM to evaluate the date of occurrence of intense rainfall events is performed on data spanning from 1998 onwards. The period coincides with the duration of the tropical rainfall measurement and GPM missions.

TRMM provides a range of rainfall products. In this work we analyze the TMPA (TRMM multi-satellite precipitation analysis) 3B42 v.7 precipitation dataset. TMPA rainfall estimates are obtained by combining TRMM PR, passive microwave (PMW), and infrared estimates within a 3 h window centered on a synoptic time (0, 3, 6, 12, 21 UTC) over the 50°S–50°N area (for more details, see [22]). From October 2014, with the decommissioning of the PR, a climatologically calibrated/adjusted research TMPA is available [23]. TMPA rainfall has high spatial (0.25 °) and temporal (3 h) resolution and is widely applied in different branches of the Earth sciences, especially in data-sparse regions (e.g., [24–27]).

From 1 April 2014 the analysis also includes the final post-real-time run of 3IMERGHH product from the GPM mission. This product is characterized by a finer spatial resolution (0.1°) and is generated on half-hourly intervals (0, 0:30, 1, 1:30, …, 23:30 UTC), over the 60°S–60°N region (for more details, see [28]). At the time of writing the product is available until 30 June 2015.

To evaluate the impact of the varying spatial resolution, 3IMERGHH products are considered at both their natural spatial resolution (0.1° × 0.1°) and at coarse resolutions of 0.2° × 0.2° and 0.3° × 0.3°.

The NOAA-GHCND rainfall dataset v 3.22 [29] is adopted; it contains daily records from over 75000 stations in 179 countries [30]. By using a 'trading space for time approach' [31, 32], such a wide and global dataset allows us to overcome the lack of robustness, which is due to the limited length of the available GPM series.

Before being aggregated to the daily scale, satellite data at the original time resolution are shifted to best match the rain gauge data, considering the combined

Table 1. Periods of the analysis and characteristics of the satellite products. The '*N* cells' field refers to the number of cells considered (i.e. the number of cells containing at least 1 rain gauge). The 3IMERGHH dataset is analyzed at the original spatial resolution (0.1°) and at coarser resolution of 0.2° and 0.3°.

Period	Dates	Product	Source	Resolution	Coverage	*N* cells
(I)	01 January 1998 31 December 2013	TMPA 3B42 v.7	TRMM	0.25°–3 h	50°S–50°N	17877
(II)	01 April 2014	TMPA 3B42 v.7	TRMM	0.25°–3 h	50°S–50°N	13808
	30 June 2015	3IMERGHH	GPM 0.1	0.10°–0.5 h	60°S–60°N	24762
		3IMERGHH	GPM 0.2	0.20°–0.5 h	60°S–60°N	17746
		3IMERGHH	GPM 0.3	0.30°–0.5 h	60°S–60°N	13140

effect of time zones and national sampling practices. When the latter is not available, we select the best match compatible with the time zone shift through a robust statistical approach, carried out at the national scale. Figure S1 displays the locations of the considered stations. Only those stations which have recorded at least 30 d of data in the 1998–2015 period are considered. Figure S1 also shows the distribution of stations per latitude interval.

In order to consider the different temporal coverage of the analyzed products, the analysis is carried out for two different time periods: (I) 1 January 1998–31 December 2013, for which only TRMM products are available; (II) 1 April 2014–30 June 2015 for which GPM products are also analyzed. A brief summary of the characteristics of the analyzed products is reported in table 1 for each period.

The analysis is carried out on a gridded domain. The cell size is set to the spatial resolution of the considered satellite product (see table 1). Each rain gauge is assigned to the related cell, according to its position. In case of cells with multiple records in a day, the largest value is considered (i.e., if multiple rain gauges belong to one cell, we only consider the maximum rainfall depth recorded each day).

For each year and cell, the N_{tot} most significant daily events identified in the satellite annual time series are compared with the N_g most significant ones recorded by the rain gauges. The dates of the occurrence of these events are now referred to as 'satellite significant dates' and 'rain gauge significant dates', respectively.

We set the value of $N_{tot} = 5$ through a preliminary analysis on a subset of the data, aimed at increasing the robustness of the results and limiting the noise in the procedure. On the other hand, we let the number N_g vary, simultaneously for all cells, between 5 and 15 in order to test the sensitivity of the results.

The agreement between the two sets of dates is then evaluated by checking how many satellite events among N_{tot} find a counterpart in the gauge-recorded significant events. In order to check the quality of the timing assessment, we consider the probability of detection [33], defined as the fraction of significant dates correctly matched over the total:

$$POD_{N_g} = N_{match}/N_{tot} \quad (1)$$

where N_{match} is the number of satellite significant dates matching the rain gauge significant dates, and N_{tot} is the number of satellite significant events considered. The probability of detection varies with the number N_g of gauge significant events considered. The range is 0–1 and the optimal value is 1.

The POD_{N_g} is evaluated for each N_g value. N_g is used as a proxy to represent the precision of the matching. The increase of N_g leads to an increase in the probability of a match and, for a given probability, to a decreased ability of the instrument to identify the right timing. The assessment of this sensitivity is deemed useful to explore the potential of satellite data and to provide the best grounds for improvements.

3. Results and discussion

Figure 2(a) shows the relationship between the average POD_{N_g} among all cells and N_g for the different analyzed products, according to the periods described in table 1. Results relating to period (I) are presented as box plots, representing the variation within the time span of the average POD_{N_g} among all cells. For period (II) lines representing the average POD_{N_g} among all cells along the whole period are plotted for the different products.

We observe that for period (I) the use of TRMM data provides a match between 'satellite significant dates' and 'rain gauge significant dates' for approximately 35% of the dates. The match rate increases, as expected, with the increase in N_g, exceeding 50% when the 15 most significant events are considered.

For period (II), over the whole range of considered N_g, GPM shows a match rate which is circa 5% greater than that of TRMM. This is a significant result, considering that the 3IMERGHH product is at the preliminary stage of its development and that, similarly to the TRMM example, refinements of the conversion algorithms and improvement in the satellite constellation equipment, will increase quality as the GPM mission moves forward [22, 34, 35]. Indeed, while the

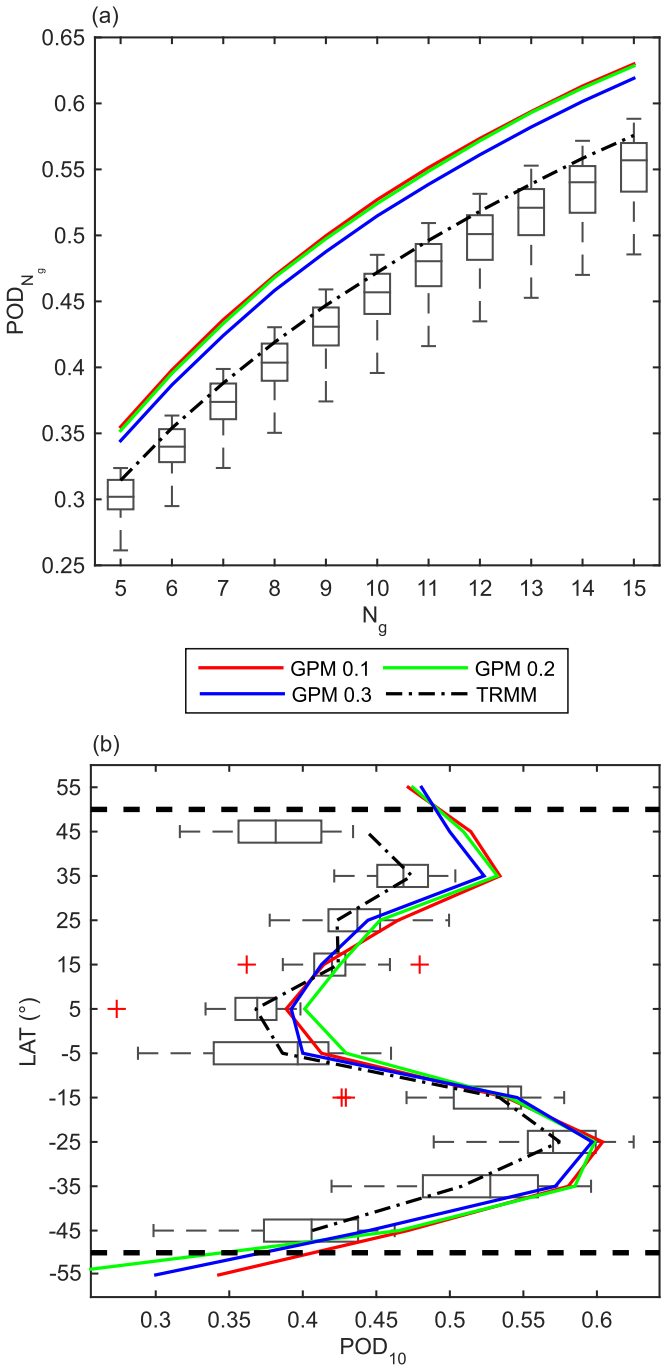

Figure 2. (a) Values of POD_{N_g} for different satellite products varying N_g. The box plots refer to the distribution of the average POD_{N_g} among all the considered cells for TRMM, along period (I). The lines refer to TRMM and GPM for period (II). GPM data are analyzed at the original resolution (0.1°) and at the coarse 0.2° and 0.3° resolutions. (b) Variability along latitude of POD_{10}, considering 10° latitude bands. The box plots refer to the distribution of the average POD_{10} among the cells of each band for TRMM, along period (I). The lines refer to TRMM and GPM in each latitude interval for period (II). GPM data are analyzed at the original resolution (0.1°) and at the coarse 0.2° and 0.3° resolutions. For both the panels the central mark of the box plots is the median, the edges of the boxes are q_1 and q_2 (i.e. the 25th and 75th percentiles), the whiskers extend to the most extreme data points not considered outliers (i.e. values out of the range $[q_3 + 1.5(q_3 - q_1), q_1 - 1.5(q_3 - q_1)]$). Outliers are plotted individually as red crosses.

shape of the box plots of TRMM annual performances in figure 2(a) seems to suggest little variation over time, a substantial improvement can be detected in TRMM performance over the years. The line referring to TRMM performance in period (II) is always above the 75th percentile of the box plots, which suggests an improvement over time. The increasing linear trend in the mean POD_{N_g} value is confirmed by a student-T test with a 5% significance level. This leads to an average of 10% increase in the ability to detect the timing of severe rainfall from the beginning to the end of the TRMM life-cycle. This improvement is singularly due to the evolution of the TRMM constellation, since the impact of the refinements in the algorithm is null given that we only consider the latest version (i.e. version 7). The variation of the distribution of the average

POD_{N_g} value along the 1998–2014 period is illustrated in figure S2. Visible improvements can be noticed corresponding to major additions and upgrades in the TRMM satellite constellation (e.g., the start of Sounding Units in 2000, etc [22]). The comparison with the median value of POD_{N_g} for GPM in period (II) highlights the potential of the instrument. If further improvements were to be obtained during the GPM mission, the probability of detection for $N_g = 5$ would draw near to a 50% accuracy.

Moreover, the comparison between the different analyzed GPM resolutions (figure 2(a)) shows that the degradation in the accuracy due to the increase in spatial resolution is negligible. This allows one to use the finest available resolution and exploit all capabilities of the instrument.

The second stage of our analysis is focused on the variability of the timing accuracy on a spatial scale. In order to reduce the complexity, the value of N_g is fixed to 10. At first, the domain is divided into latitude bands of 10°. The POD_{10} is then evaluated for each interval. Box plots representing the variation within period (I) of the average POD_{10} among the cells in each latitude band are shown in figure 2(b). For period (II) the mean value of the POD_{10} for each latitude band is reported.

Both TRMM and GPM show an evident variability with latitude, with maxima in the correspondence of latitudes 35°N and 25°S and minima at the Equator and at the borders of GPM and TRMM domains. The fluctuation of the POD_{10} with latitude shows significant similarities with the distribution of the rain gauges (figure S1). Both results show a concurring double-peaked behavior; the areas characterized by greater rain gauge densities seem to display larger POD_{10}. This outcome can be partially attributed to a greater robustness of the results in areas with higher rain gauge densities, where POD_{10} is less sensitive to outliers. A higher density coincides with a larger probability of having multiple rain gauges in the same cell. This provides longer gauge series for comparisons, and facilitates the identification of the significant events. Moreover, the areas with higher rain gauge densities coincide with the countries that provide more frequent updates of rainfall data (e.g., USA, Australia). Low density areas (e.g., at the Equator) are more sensitive to outliers, and the lack of complete series complicates the identification of the top events by adding noise to the system. The Equatorial band in figure 2(b) presents a lesser degradation, even if minimal, with the coarser GPM resolution compared to the original one. A coarse spatial resolution can probably allow for a more robust verification by attenuating the negative effects of the smaller gauge density (i.e. it allows for multiple rain gauges in the same cell, even in the presence of low densities). The main issues identified could therefore be attributed more likely to the dataset used in the verification phase than to a real decrease in the detection performance. Further investigations are thus recommended at the latitudes with a low gauge density, as soon as a denser dataset will be available, since the current status does not allow for further analysis.

The spatial distribution at the global scale of the POD_{10} for TRMM on period (I) and for TRMM and GPM on period (II) is presented in figure 3. The resolution, at $5^\circ \times 5^\circ$, is coarse because of the difficulty to distinguish isolated cells at the original resolution. In period (I) (panel (a)), the results are consistent with what emerges from figure 2(b), presenting a cluster of larger POD_{10} values around Oceania. POD_{10} values are of the order of 0.45 even in areas characterized by deep convection, in which TRMM products are known to be unreliable (e.g., South American Andes [5]). The cluster of small POD_{10} values located in Brazil is probably due to the worse local quality of the rain gauge data. In fact, from figure S1, one notices that the data availability for the region is limited to a single year. Once again, table 2 confirms that TRMM results show large improvements when considering solely period (II).

Panels (b) and (c) of figure 3 represent respectively the performance of TRMM and GPM over period (II). For ease of comparison figure S3 presents a map of the differences between the POD_{10} with GPM and the POD_{10} with TRMM. The results of the two instruments seem generally consistent, with large areas with coincident POD_{10} values. Some areas in which TRMM seems to exceed GPM are clearly identifiable (e.g, Bolivia, Indian area). On the other hand, noticeable improvements can be recognised in areas where global satellite products are known to be poorly reliable (e.g, Europe and Mediterranean Area). As the comparison is difficult due to the complex spatial variability, results are summarised for some areas of interest in table 2. This confirms remarkable improvements for GPM at the global scale, allowing for an increase in the POD_{10} up to 10% for the Mediterranean basin and Africa.

The value of N_g was set beforehand at a fixed value; this assumption has proven acceptable because, in the context of the analysis of the spatial variation, N_g turns out to be a less significant parameter. Even though different values of N_g produce different absolute values of POD_{N_g}, the global trend in the spatial pattern is preserved. For completeness, the analogues of figures 2(b) and 3 for $N_g = 5$ are included as figure S4 and figure S5. Despite the differences in the magnitude, the spatial distributions are similar.

4. Conclusions

Satellite rainfall products have been analyzed in order to assess their potential in describing severe precipitation events at the global scale. Satellite products are known to underestimate rainfall rates for deep convective systems. However, their high spatio-temporal resolution and their quasi-global coverage make them

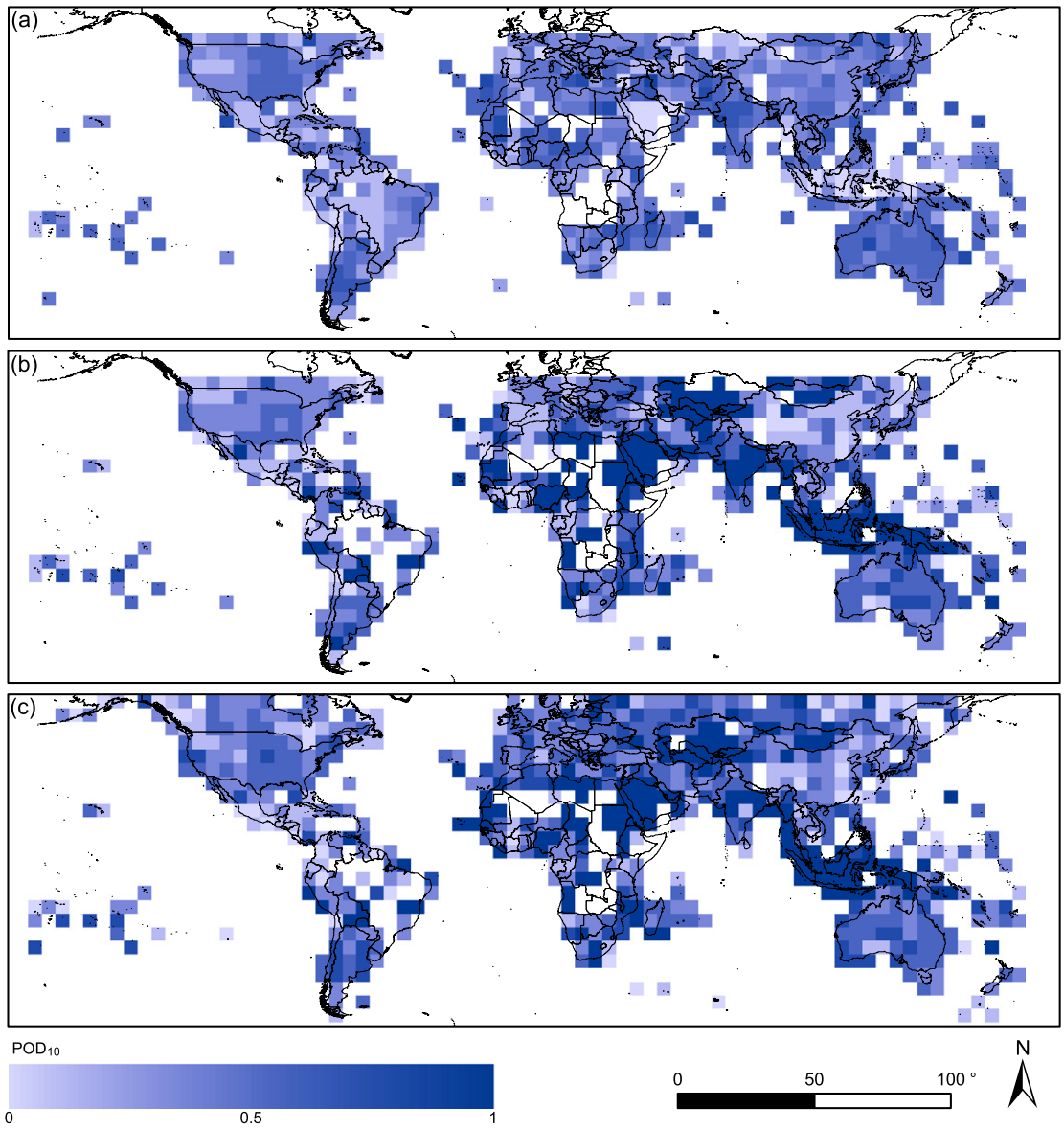

Figure 3. Average POD_{10} on a 5° × 5° gridded domain. (a) TRMM over period (I) and (b) over period (II). (c) GPM at the original resolution over period (II).

Table 2. Mean and standard deviation of the distribution of the POD_{10} for some areas of interest.

	Period (I)		Period (II)			
	TRMM		TRMM		GPM 0.1	
	Mean	St.dev.	Mean	St.dev.	Mean	St.dev.
Africa	0.44	0.17	0.53	0.33	0.62	0.31
America (North)	0.44	0.15	0.47	0.25	0.53	0.26
America (Center-South)	0.38	0.18	0.49	0.30	0.49	0.31
Asia (West)	0.43	0.15	0.55	0.32	0.59	0.32
Asia (Middle-East)	0.39	0.20	0.61	0.35	0.66	0.32
Europe	0.36	0.16	0.44	0.27	0.51	0.24
Oceania	0.54	0.11	0.54	0.24	0.59	0.24
Andes	0.45	0.18	0.52	0.31	0.54	0.32
Australia	0.54	0.11	0.55	0.24	0.59	0.24
Brazil	0.37	0.18	0.56	0.31	0.65	0.34
Mediterranean basin	0.37	0.18	0.43	0.29	0.53	0.27
USA	0.45	0.14	0.48	0.24	0.54	0.26

useful in the definition of spatial precipitation features.

A preliminary analysis carried out in the Liguria Region (North-West of Italy) confirms a marked underestimation of extreme rainfall depths, but highlights the ability of TRMM to identify the dates of occurrence of severe rainfall events.

The analysis is expanded to the global scale, considering the NOAA-GHCND rainfall dataset v 3.22 [29] over the 1998–2015 period. The performance of TRMM in identifying the timing of global extreme precipitations is found consistent with that obtained in the preliminary analysis, matching nearly 35% of the dates of occurrence. The matching capability registers a 10% improvement over the TRMM life-cycle due to the evolution of the satellite constellation.

The results shown by the GPM mission after just one year of operation seem promising. The finer spatio-temporal resolution and the increased measurement range (to include light-intensity precipitation and falling snow [36]) allow GPM results to be more accurate than TRMM ones. At the global scale GPM products show a greater ability in matching the day of occurrence of intense rainfall, with a probability of detection in the order of 0.6–0.7. These results hold also for the areas in which TRMM faces issues due to the flattening of the rainfall peaks (e.g., the Mediterranean region). Having proven that the time-detecting ability is not affected by a higher resolution, the finer spatial scales can be used for a more accurate analysis.

The great abundance of data considered in the present work leads to significant outcomes concerning the limits of TRMM products in the analysis of intense rainfall events and the high potential that GPM shows after just one year of operation. Nevertheless, further in-depth analysis is needed in areas of low gauge density which impedes a proper assessment of the results.

Satellite data can play an important role in the analysis of the spatio-temporal connection between severe rainfall systems at the global scale. The timing identification approach can provide new perspectives for the use of satellite products for the analysis of extreme rainfall, since the lack of accuracy at the daily scale hinders its direct systematic use. All in all, the global nature of satellite data allows the analysis of precipitation systems in regions with limited or absent ground records. Further studies, which are certainly needed, can help opening new horizons for the hydrologic design and planning in remote parts of the world.

Acknowledgments

This work is partially funded by the Australian Research Council. The authors wish to thank Dr George J Huffman for the useful discussion on the results and the two anonymous reviewers for their valuable comments and suggestions to improve the quality of the paper. Regione Liguria is acknowledged for providing data from the regional meteorological observational network, available on the institutional website http://cartografiarl.regione.liguria.it/SiraQualMeteo/Fruizione.asp. TRMM and GPM data are available on the dedicated page of the NASA website via http://pmm.nasa.gov/data-access. NOAA-GHCND dataset v 3.22 is available in [29].

References

[1] Fiori E, Comellas A, Molini L, Rebora N, Siccardi F, Gochis D, Tanelli S and Parodi A 2014 Analysis and hindcast simulations of an extreme rainfall event in the Mediterranean area: the Genoa 2011 case *Atmos. Res.* **138** 13–29

[2] Chappell C F 1986 Quasi-stationary convective events *Mesoscale Meteorology and Forecasting* ed P S Ray (Boston, MA: American Meteorological Society) pp 289–310

[3] Hasan M M, Sharma A, Johnson F, Mariethoz G and Seed A 2014 Correcting bias in radar *Z–R* relationships due to uncertainty in point rain gauge networks *J. Hydrol.* **519** 1668–76

[4] Delrieu G *et al* 2005 The catastrophic flash-flood event of 8–9 September 2002 in the Gard region, France: a first case study for the Cévennes–Vivarais Mediterranean hydrometeorological observatory *J. Hydrometeor* **6** 34–52

[5] Rasmussen K L, Choi S L, Zuluaga M D and Houze R A 2013 TRMM precipitation bias in extreme storms in South America *Geophys. Res. Lett.* **40** 3457–61

[6] Cai Y, Jin C, Wang A, Guan D, Wu J, Yuan F and Xu L 2015 Spatio-temporal analysis of the accuracy of tropical multisatellite precipitation analysis 3B42 precipitation data in mid-high latitudes of China *PLoS One* **10** e0120026

[7] Ochoa A, Pineda L, Willems P and Crespo P 2014 Evaluation of TRMM 3B42 (TMPA) precipitation estimates and WRF retrospective precipitation simulation over the Pacific-Andean basin into Ecuador and Peru *Hydrol. Earth Syst. Sci. Discuss.* **11** 411–49

[8] Lo Conti F, Hsu K L, Noto L V and Sorooshian S 2014 Evaluation and comparison of satellite precipitation estimates with reference to a local area in the Mediterranean Sea *Atmos. Res.* **138** 189–204

[9] Romilly T G and Gebremichael M 2011 Evaluation of satellite rainfall estimates over Ethiopian river basins *Hydrol. Earth Syst. Sci* **15** 1505–14

[10] Fleming K, Awange J, Kuhn M and Featherstone W 2011 Evaluating the TRMM 3B43 monthly precipitation product using gridded raingauge data over Australia *Aust. Meteorol. Oceanographic J.* **61** 171–84 (www.bom.gov.au/amoj/papers.php?year=2011)

[11] Zulkafli Z, Buytaert W, Onof C, Manz B, Tarnavsky E, Lavado W and Guyot J L 2014 A comparative performance analysis of TRMM 3B42 (TMPA) versions 6 and 7 for hydrological applications over Andean-Amazon river basins *J. Hydrometeor* **15** 581–92

[12] Ward E, Buytaert W, Peaver L and Wheater H 2011 Evaluation of precipitation products over complex mountainous terrain: a water resources perspective *Adv. Water Resour.* **34** 1222–31

[13] Dinku T, Connor S J and Ceccato P 2010 Comparison of CMORPH and TRMM-3B42 over mountainous regions of Africa and South America *Satellite Rainfall Applications for Surface Hydrology* ed M Gebremichael and F Hossain (Netherlands: Springer) pp 193–204

[14] Iguchi T, Kozu T, Kwiatkowski J, Meneghini R, Awaka J and Okamoto K 2009 Uncertainties in the rain profiling algorithm for the TRMM precipitation radar *J. Meteorol. Soc. Japan* A **87** 1–30

[15] Tian Y and Peters-Lidard C D 2010 A global map of uncertainties in satellite-based precipitation measurements *Geophys. Res. Lett.* **37** L24407

[16] Hou A Y, Kakar R K, Neeck S, Azarbarzin A A, Kummerow C D, Kojima M, Oki R, Nakamura K and Iguchi T

2014 The global precipitation measurement mission *Bull. Am. Meteorol. Soc.* **95** 701–22
[17] Cleveland W S and Devlin S J 2011 Locally weighted regression: an approach to regression analysis by local fitting *J. Am. Stat. Assoc.* **83** 596–610
[18] Su F, Hong Y and Lettenmaier D P 2008 Evaluation of TRMM multisatellite precipitation analysis (TMPA) and its utility in hydrologic prediction in the La Plata basin *J. Hydrometeor* **9** 622–40
[19] Flocas H A, Simmonds I, Kouroutzoglou J, Keay K, Hatzaki M, Bricolas V and Asimakopoulos D 2010 On cyclonic tracks over the eastern mediterranean *J. Clim.* **23** 524–57
[20] Vrieling A, Hoedjes J C B and Van der Velde M 2014 Towards large-scale monitoring of soil erosion in Africa: accounting for the dynamics of rainfall erosivity *Glob. Planet. Change* **115** 33–43
[21] Coe J A, Michael J A, Crovelli R A, Savage W Z, Laprade W T and Nashem W D 2004 Probabilistic assessment of precipitation-triggered landslides using historical records of landslide occurrence *Environ. Eng. Geosci.* **10** 103–22
[22] Huffman G J, Bolvin D T, Nelkin E J, Wolff D B, Adler R F, Gu G, Hong Y, Bowman K P and Stocker E F 2007 The TRMM multisatellite precipitation analysis (TMPA): quasi-global, multiyear, combined-sensor precipitation estimates at fine scales *J. Hydrometeor* **8** 38–55
[23] Bolvin D and Huffman G 2015 *Transition of 3B42/3B43 Research Product from Monthly to Climatological Calibration/ Adjustment* (Washington, DC: NASA)
[24] Awadallah A G and Awadallah N A 2013 A novel approach for the joint use of rainfall monthly and daily ground station data with TRMM data to generate IDF estimates in a poorly gauged arid region *Open J. Modern Hydrol.* **03** 1–7
[25] Khan S I, Adhikari P, Hong Y, Vergara H, Adler R F, Policelli F, Irwin D, Korme T and Okello L 2011 Hydroclimatology of Lake Victoria region using hydrologic model and satellite remote sensing data *Hydrol. Earth Syst. Sci.* **15** 107–17
[26] Asante K O, Arlan G A, Pervez S and Rowland J 2008 A linear geospatial streamflow modeling system for data sparse environments *Int. J. River Basin Manage.* **6** 233–41
[27] Bindlish R, Jackson T J, Wood E, Gao H, Starks P, Bosch D and Lakshmi V 2003 Soil moisture estimates from TRMM microwave imager observations over the southern United States *Remote Sens. Environ.* **85** 507–15
[28] Huffman G J, Bolvin D T and Nelkin E J 2014 *Integrated Multi-satellitE Retrievals for GPM* (*IMERG*) *Technical Documentation* (Washington, DC: NASA)
[29] Menne M J *et al* 2012 *Global Historical Climatology Network-Daily* (*GHCN-Daily*), *Version 3. 22* (NOAA National Climatic Data Center) (http://1.ncdc.noaa.gov/pub/data/ghcn/daily/)
[30] Menne M J, Durre I, Vose R S, Gleason B E and Houston T G 2012 An overview of the global historical climatology network-daily database *J. Atmos. Ocean. Technol.* **29** 897–910
[31] Singh R, Wagener T, van Werkhoven K, Mann M E and Crane R 2011 A trading-space-for-time approach to probabilistic continuous streamflow predictions in a changing climate-accounting for changing watershed behavior *Hydrol. Earth Syst. Sci.* **15** 3591–603
[32] Peel M C and Bloschl G 2011 Hydrological modelling in a changing world *Prog. Phys. Geography* **35** 249–61
[33] Wilks D S 2011 *Statistical Methods in the Atmospheric Sciences* (*International Geophysics Series* vol 91) ed R Dmowska *et al* (Burlington, MA: Academic)
[34] Zhong L 2015 Comparison of versions 6 and 7 3 hourly TRMM multi-satellite precipitation analysis (TMPA) research products *Atmos. Res.* **163** 91–101
[35] Kummerow C *et al* 2000 The status of the tropical rainfall measuring mission (TRMM) after two years in orbit *J. Appl. Meteorol.* **39** 1965–82
[36] Mugnai A *et al* 2007 Snowfall measurements by proposed European GPM mission *Measuring Precipitation from Space: EURAINSAT and the Future* (*Advances In Global Change Research* vol 28) ed V Levizzani *et al* (Netherlands: Springer) pp 655–74